



A Journal of the Gesellschaft Deutscher Chemiker

Angewandte Chemie

GDCh

International Edition

www.angewandte.org

Accepted Article

Title: Precision molecular threading/dethreading

Authors: Jessica Groppi, Lorenzo Casimiro, Martina Canton, Stefano Corra, Mina Jafari-Nasab, Gloria Tabacchi, Luigi Cavallo, Massimo Baroncini, Serena Silvi, Ettore Fois, and Alberto Credi

This manuscript has been accepted after peer review and appears as an Accepted Article online prior to editing, proofing, and formal publication of the final Version of Record (VoR). This work is currently citable by using the Digital Object Identifier (DOI) given below. The VoR will be published online in Early View as soon as possible and may be different to this Accepted Article as a result of editing. Readers should obtain the VoR from the journal website shown below when it is published to ensure accuracy of information. The authors are responsible for the content of this Accepted Article.

To be cited as: *Angew. Chem. Int. Ed.* 10.1002/anie.202003064

Link to VoR: <https://doi.org/10.1002/anie.202003064>

Precision molecular threading/dethreading

Jessica Groppi,^[a] Lorenzo Casimiro,^[a,b] Martina Canton,^[a,c] Stefano Corra,^[a,d] Mina Jafari-Nasab,^[b] Gloria Tabacchi,^[e] Luigi Cavallo,^[f] Massimo Baroncini,^[a,d] Serena Silvi,^[a,b] Ettore Fois,^{*,[e]} and Alberto Credi^{*,[a,c]}

[a] Dr. J. Groppi,^[*] L. Casimiro,^[*] M. Canton, Dr. S. Corra, Dr. M. Baroncini, Prof. S. Silvi, Prof. A. Credi
CLAN–Center for Light Activated Nanostructures, Istituto ISOF-CNR
via Gobetti 101, 40129 Bologna, Italy.

[*] Equal contribution.

[b] L. Casimiro, M. Jafari-Nasab, Prof. S. Silvi
Dipartimento di Chimica “G. Ciamician”, Università di Bologna
via Selmi 2, 40126 Bologna, Italy.

[c] M. Canton, Prof. A. Credi
Dipartimento di Chimica Industriale “Toso Montanari”, Università di Bologna
viale del Risorgimento 4, 40136 Bologna, Italy
E-mail: alberto.credi@unibo.it

[d] Dr. S. Corra, Dr. M. Baroncini
Dipartimento di Scienze e Tecnologie Agro-alimentari, Università di Bologna
viale Fanin 44, 40127 Bologna, Italy

[e] Prof. G. Tabacchi, Prof. E. Fois
Dipartimento di Scienza ed Alta Tecnologia and INSTM, Università dell’Insubria
via Valleggio 11, 22100 Como, Italy.
E-mail: etttore.fois@uninsubria.it

[f] Prof. L. Cavallo
KAUST Catalysis Center, King Abdullah University of Science and Technology,
Thuwal 23955-6900, Saudi Arabia.

Supporting information for this article is given via a link at the end of the document.

Abstract: The general principles guiding the design of molecular machines based on interlocked structures are well known. Nonetheless, the identification of suitable molecular components for a precise tuning of the energetic parameters that determine the mechanical link is still challenging. Indeed, what are the reasons of the “all-or-nothing” effect, which turns a molecular “speed-bump” into a stopper in pseudorotaxane-based architectures? Here we investigate the threading and dethreading processes for a representative class of molecular components, based on symmetric dibenzylammonium axles and dibenzo[24]crown-8 ether, with a joint experimental-computational strategy. From the analysis of quantitative data and an atomistic insight, we derive simple rules correlating the kinetic behaviour with the substitution pattern, and provide rational guidelines for the design of modules to be integrated in molecular switches and motors with sophisticated dynamic features.

Introduction

In the macroscopic world, engineering a proper fitting between the component parts is key for the design of any static or dynamic mechanical structure. In general, this is also true at the nanoscale, wherein molecules can be tailored to behave as building blocks for the construction of supramolecular architectures with valuable structural or functional properties.^[1,2] The parts commonly used to build macroscopic structures are made of hard materials with well-defined mechanical properties. Conversely, molecules are floppy (because of the softness of the potential energy profiles that determine bond lengths and angles) and sticky (because of the presence of attractive intermolecular forces, including the ubiquitous van der Waals interactions) objects, in which steric and electronic effects are intimately connected. Inertial effects are negligible for molecules

because of their tiny mass and movement at ambient temperature is dominated by thermal agitation.^[2c, 3] Another significant difference between a macroscopic and a nanoscale structure is that, for the latter, the surrounding medium consists of objects (*i.e.*, molecules) of approximately the same size of the structure itself. The interlocking of molecular components^[4] is the concept at the basis of the mechanical bond, which in the past three decades has enabled the development of mechanically interlocked molecules, an entirely new class of compounds endowed with highly appealing structural and dynamic properties.^[5] Of particular interest in this regard are the rotaxanes, *i.e.*, species composed minimally of a macrocycle surrounding a dumbbell-shaped molecule. Rotaxanes are usually obtained by self-assembly of complementary ring and axle molecular components to obtain a threaded supramolecular complex (pseudorotaxane), and successively attaching bulky groups (stoppers) at the extremities of the axle to prevent the escape of the ring. The efficacy of the mechanical interlocking is determined by the energy barrier for dethreading which, in turn, depends on the bulkiness of the stoppers, the flexibility of the ring, and the possible presence of electronic interactions that could change the energetic barrier to (de)threading. Indeed, the possibility of adjusting the threading and dethreading barriers by molecular design, and modulating the corresponding rates by temperature changes, highlights the ill-defined nature of pseudorotaxanes,^[6] and has been successfully exploited to self-assemble rotaxanes by the so-called slippage route (Figure 1).^[7, 8] Besides size complementarity, other approaches examined for affecting (de)threading rates rely on electrostatic effects^[9] and on the conformational freedom of long threads.^[10] (Pseudo)rotaxanes endowed with end groups that can change their size and shape upon external (*e.g.*, light) stimulation have also been reported.^[11]

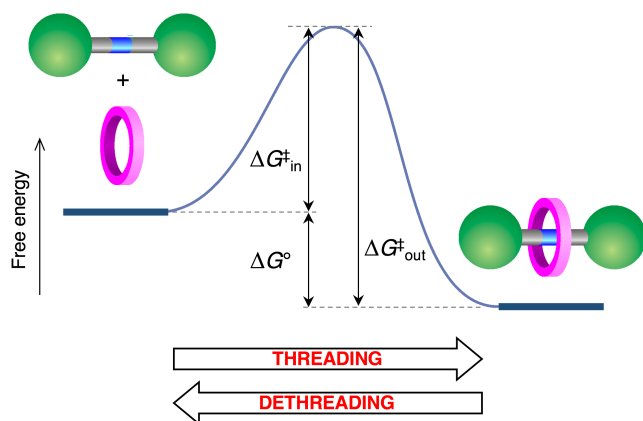


Figure 1. Schematic potential energy profile describing the threading and dethreading of molecular ring- and dumbbell-shaped components to yield (pseudo)rotaxanes.

The energy barriers associated with the relative movement of threaded ring and axle components are also of paramount importance for the construction of molecular motors based on rotaxanes and related systems.^[1a,2c, 12] The directionally controlled movements that take place in a molecular motor can only be obtained with the application of ratchet mechanisms that bias (that is, rectify) random thermal motion via the stimuli-controlled modulation of the energy wells and barriers that describe the intercomponent movements.^[2c,13] In other words, a time-dependent potential landscape with repeating asymmetric features is required to break the spatial and time-reversal symmetries along the direction of motion and establish directional control. This approach was ingeniously implemented on catenanes to make rotary motors,^[14] and its potentialities are well exemplified by the recent development of supramolecular pumps – systems in which macrocyclic rings can be moved directionally along an oriented axle under chemical,^[15] electrical^[16] or light^[17] energy supply. Although the current systems operate in solution, wherein exploiting the transport to perform a function is very challenging, the natural development of this research is towards systems that can operate in compartmentalized environments – for example, membrane-separated solutions – in which the molecular pumping can lead to, e.g., the buildup of a concentration gradient that can subsequently be harnessed.^[18]

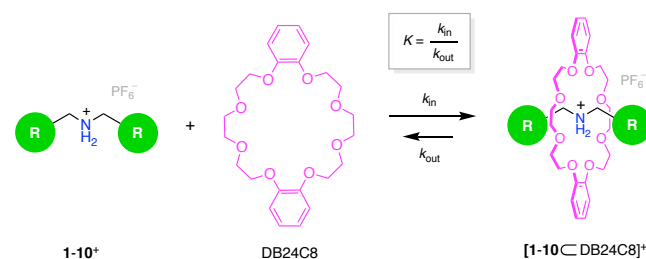
A precise engineering of the energy barriers associated with relative ring-axle movements in (pseudo)rotaxanes is indeed crucial for the design of such novel functional supramolecular pumps,^[11b,15,17, 19] as well as dynamic polymeric materials containing mechanical bonds.^[20] Despite the huge amount of work performed on self-assembled ring-and-axle complexes in terms of stability,^[5,21] systematic analyses on the threading and dethreading rates of pseudorotaxanes are relatively rare in the literature.^[6,7,11c,22] These studies highlighted the complexity of these phenomena and showed that, even in the absence of electrostatic effects, size complementarity of ring and stopper should be used with caution as a criterion for interpreting (de)slipping processes.^[22b,g] It is therefore not surprising that the problem of designing supramolecular complexes and related interlocked species that exhibit intercomponent mobility with predetermined kinetics is usually tackled with an empirical approach. This work lays down a knowledge-based design


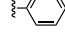
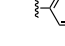

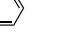
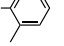

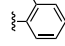
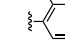
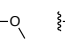
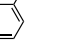
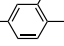
strategy by dissecting the threading and dethreading processes of a series of symmetric dibenzylammonium ions, bearing different substituents, with dibenzo[24]crown-8 ether (DB24C8) in CH_2Cl_2 . The choice of this particular self-assembling architecture^[23] is dictated primarily by its widespread popularity in supramolecular chemistry^[1,2,5,24,25] and related applications,^[26] that include self-assembled materials,^[27] catalysis,^[28] and molecular switches and motors.^[17,18, 29] By combining experimental and computational techniques, we unravel the molecular-level factors that govern with atomistic precision the corresponding energy barriers. Finally, we derive general guidelines for the rational identification of (pseudo)stopper components that can be useful for designing novel molecular-based devices, machines and materials based on mechanically interlocked molecules and supramolecular counterparts.

Results and Discussion

Design and synthesis of the components

The investigated compounds are summarized in Scheme 1. The ring is DB24C8, and the dumbbell-shaped guests are symmetric dibenzylammonium-type cations (hexafluorophosphate salts) bearing methoxy and/or methyl substituents on either phenyl ring. The driving force for the formation of the threaded complexes in low polarity solvents arises essentially from $[\text{N}^+ \cdots \text{H} \cdots \text{O}]$ and $[\text{C} \cdots \text{H} \cdots \text{O}]$ hydrogen bonds, with a contribution from π - π stacking interactions involving the phenyl rings.^[6a,21,22a,23] Indeed, the minimum energy structures calculated for two representative compounds in the gas phase (Figure 2 and SI) suggest that the threaded complexes are thermodynamically stable. To maximize π - π stacking, the ring adopts a chair conformation (Figure 2b,e) while its elliptical cavity perfectly fits to the central part of the axle, constituted by the $-\text{CH}_2\text{NH}_2^+\text{CH}_2-$ moiety. This arrangement allows both the ammonium hydrogen atoms to form hydrogen bonds with the oxygen atoms of DB24C8, while the $-\text{CH}_2-$ groups are engaged in weaker $[\text{C} \cdots \text{H} \cdots \text{O}]$ interactions (see the SI, Figure S1).



| | | | | | |
|---|---|--|---|---|---|
|  |  |  |  |  |  |
| Cmpd. | 1 ⁺ | 2 ⁺ | 3 ⁺ | 4 ⁺ | 5 ⁺ |
|  |  |  |  |  |  |
| Cmpd. | 6 ⁺ | 7 ⁺ | 8 ⁺ | 9 ⁺ | 10 ⁺ |

Scheme 1. Structure formulas of the investigated molecular components and their self-assembly into (pseudo)rotaxane species.

Because of the structural similarity, we envisioned that guests **1–10**⁺ could exhibit (i) a comparable thermodynamic affinity for DB24C8 and (ii) similar solubility properties, thus constituting a homogeneous series of compounds to investigate the role of the terminal groups in the association and dissociation kinetics. The objective of this study is to investigate the borderline between rapidly equilibrating supramolecular complexes and kinetically inert rotaxanes. The choice of the substitution patterns shown in Scheme 1 was performed accordingly, and was guided by size complementarity considerations based on the inspection of physical molecular models.

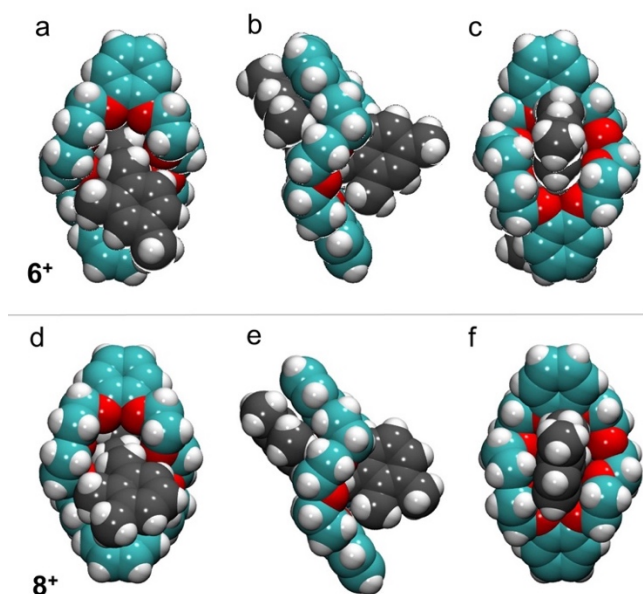


Figure 2. Space-filling representations of the minimum energy structure computed for supramolecular complexes of DB24C8 with guest **6**⁺ (a: front view; b: side view; c: back view) and with guest **8**⁺ (d: front view; e: side view; f: back view). In all structures, the $-\text{CH}_2\text{NH}_2^+\text{CH}_2-$ moiety of the axle is not visible, as it is completely encapsulated by the elliptical cavity of the ring. Atom color codes: C (ring) = cyan; C (axle) = grey; O = red; H = white.

With a similar purpose, Stoddart and coworkers studied the assembly of DB24C8 with symmetric dialkylammonium guests bearing cycloalkane end groups.^[23b] The interest of these compounds in a general context, however, is limited with respect to dibenzylammonium-type ions because of the much poorer binding with crown ethers and the nontrivial synthetic issues associated with the inclusion of cycloalkane units in the axle components of molecular machines. Conversely, the incorporation of substituted phenyl units in extended axle-type molecules appears to be a feasible way to implement kinetic barriers or “speed bumps” for ring (de)threading or shuttling.^[15,19,22a,d,e,24]

DB24C8 is commercially available, while the ammonium guests **1–10**·PF₆ were prepared by using conventional procedures; details are provided in the SI. All the experiments were performed in air equilibrated dichloromethane at room temperature (298±2 K). The choice of the solvent was dictated by the large binding constants expected in the non-competitive and apolar CH₂Cl₂.^[23b] The strong association between the components enables the use of steady-state and time-resolved

UV-visible spectroscopic measurements on dilute solutions to gain quantitative information on the thermodynamic and kinetic aspects of the self-assembly. Non-coordinating hexafluorophosphate was adopted as the counterion of the ammonium guests because it is known that, thanks to its low tendency to ion pairing, it does not affect the self-assembly in the examined concentration range.^[30]

Binding constants

¹H NMR Spectroscopy was employed to gain qualitative evidence for the formation of the complexes and to verify their threaded nature. As an illustrative example, the comparison between the separate ¹H NMR spectra in CD₂Cl₂ at room temperature of DB24C8 and thread **4**⁺ (blue line for **4**⁺ and green line for DB24C8 in Figure 3a) and of an equimolar mixture of the two (red line in Figure 3a) evidences the formation of a [2]pseudorotaxane complex characterized by a high association constant and whose (de)threading processes are slow in the NMR timescale. The new multiplet at 4.75 ppm, which appears in the spectrum of the mixture, is indicative of the involvement of the benzylic protons of **4**⁺ in hydrogen bonding with the oxygen atoms inside the cavity of the crown ether macrocycle. Moreover, the marked shielding of the aromatic protons and methyl groups of **4**⁺ confirms the presence of a significant π - π stacking interaction between the catechol moieties of DB24C8 and the phenyl groups of the thread. These observations are in full agreement with previous studies dealing with the formation of [2]pseudorotaxanes between dibenzylammonium-type threads and DB24C8.^[6a,23]

The formation of a complex was also accompanied by changes in the UV-visible absorption spectrum. Both DB24C8 and the dialkylammonium guests exhibit absorption bands in the 250-300 nm region (see the SI), which are perturbed when the components are assembled (see, e.g., Figure 3b). The absorption spectral changes were employed to determine the binding constants, *K*, by means of titrations. In the case of slow threading, particular care was taken to ensure that equilibrium had been reached for each data point during the titration experiments.

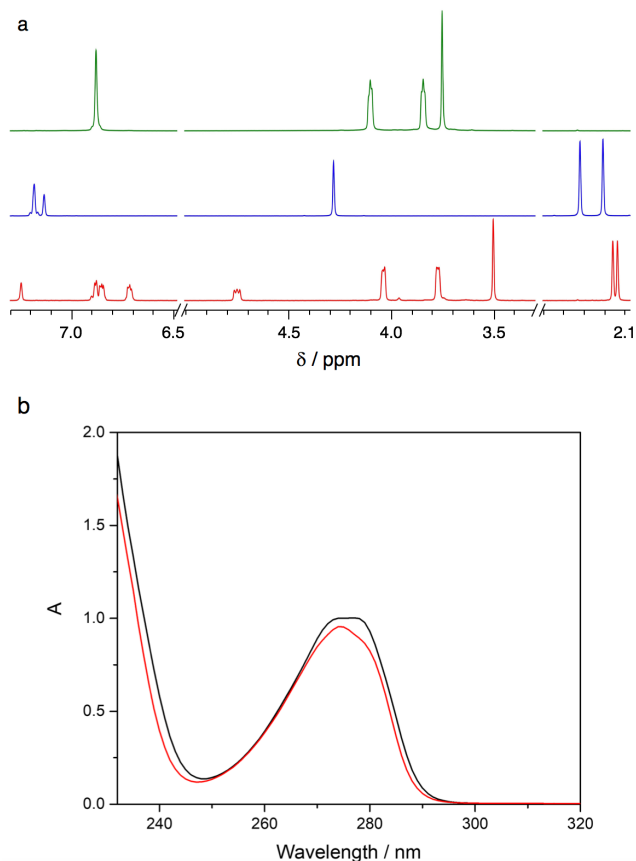


Figure 3. (a) ¹H NMR spectra (500 MHz, 298 K, CD₂Cl₂) of: 4⁺ (3.0×10⁻³ M) (blue line), DB24C8 (3.0×10⁻³ M) (green line), and a 1:1 mixture of 4⁺ and DB24C8 (both components 3.0×10⁻³ M) (red line). (b) Sum of the absorption spectra of separated CH₂Cl₂ solutions of DB24C8 and 4⁺ (black line) and absorption spectrum of the same solutions after mixing (red line). Concentrations in the mixture: [DB24C8] = 1.6×10⁻⁴ M, [4⁺] = 1.5×10⁻⁴ M.

Titration curves were performed in CH₂Cl₂ by adding small aliquots of a concentrated solution of the guest to a sub-mM solution of DB24C8. The corresponding titration curves, obtained by plotting the absorbance value at selected wavelengths (Figure 4 and SI), can be satisfactorily fitted with a least-squares nonlinear procedure according to a 1:1 binding model, in agreement with the formation of [2]pseudorotaxanes. The binding constants (Table 1), on the order of 10⁵–10⁶ L mol⁻¹, are in line with those previously determined in similar conditions for this kind of complexes.^[30]

In general, the binding constant decreases slightly, in comparison with dibenzylammonium, when the phenyl rings of the secondary ammonium guest bear methyl or methoxy substituents (1⁺ versus 4⁺, 6⁺ and 7⁺, Table 1). In line with previous observations,^[21] it can be hypothesized that the presence of electron-donor substituents lowers the hydrogen bond donor ability of the NH₂⁺ moiety and of the adjacent benzylic groups, thus diminishing the interaction with the crown ether. The association of DB24C8 with guest 9⁺ could not be studied quantitatively because, quite unexpectedly, the latter (PF₆⁻ salt) is insoluble in CH₂Cl₂. The formation of a threaded complex, though, was observed in acetonitrile by means of ¹H NMR spectroscopy. This result suggests that the 2,3-dimethylphenyl end group of 9⁺ can thread through the ring at room temperature and thus behaves as a pseudostopper.

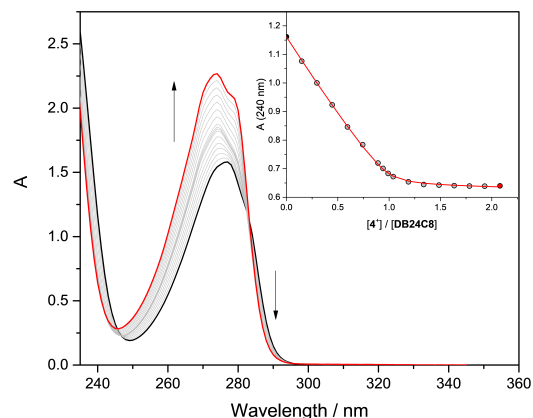


Figure 4. Absorption spectra of a 3.0×10⁻⁴ M solution of DB24C8 in CH₂Cl₂ upon addition of 4⁺. The inset shows the absorption changes at 240 nm together with the fitted curve corresponding to a 1:1 binding model.

Table 1. Thermodynamic and kinetic data (CH₂Cl₂, 298 K).

| Guest ^[a] | K (10 ⁵ L mol ⁻¹) ^[b] | k_{in} (L mol ⁻¹ s ⁻¹) ^[c] | k_{out} (s ⁻¹) ^[d] | $t_{1/2}$ (min) ^[e] |
|----------------------|---|--|---|--------------------------------|
| 1 ⁺ | 22±4 | > 2×10 ⁷ [f] | > 9 [g] | < 0.003 |
| 2 ⁺ | [h] | < 7×10 ⁻⁵ [h,i] | | |
| 3 ⁺ | [h] | < 7×10 ⁻⁵ [h,i] | | |
| 4 ⁺ | 8±3 | 37.9±0.4 | (4.7±0.5)×10 ⁻⁵ | 246 |
| 5 ⁺ | [h] | < 7×10 ⁻⁵ [h,i] | | |
| 6 ⁺ | 1.7±0.7 | 12±1 | (7.0±0.7)×10 ⁻⁵ | 165 |
| 7 ⁺ | 7±2 | 34±1 | (4.9±0.2)×10 ⁻⁵ | 236 |
| 8 ⁺ | [h] | < 7×10 ⁻⁵ [h,i] | | |
| 9 ⁺ | [j] | [j] | | |
| 10 ⁺ | [h] | < 7×10 ⁻⁵ [h,i] | | |

[a] Shaded entries highlight the axles that undergo fast threading. [b] Binding constant. [c] Threading rate constant. [d] Dethreading rate constant. [e] Half-life of the complex, calculated as $t_{1/2} = \ln 2 / k_{out}$. [f] The process is faster than the time resolution of our stopped-flow spectrometer; lower limiting value of k_{in} determined as described in the SI. [g] Estimated as $k_{out} = k_{in} / K$. [h] No complex is detected by ¹H NMR after 72 h. [i] Upper limiting value determined as described in the SI. [j] Data could not be obtained because of the poor solubility of axle 9⁺ in CH₂Cl₂. Measurements performed in acetonitrile indicate that this axle belongs to the “threading” category.

Threading and dethreading rate constants

The UV-visible spectral changes observed upon self-assembly (Figure 3b) were also employed to measure the threading rate constants, k_{in} , by monitoring the absorbance as a function of time after rapid mixing of the components in equimolar amounts. Depending on the threading time scale, the kinetic experiments were either performed by manual mixing in a normal spectrophotometer, or with a stopped-flow instrument. The threading and dethreading rate constants were determined from the fitting of the time-dependent absorbance traces (Figure 5) with an equilibrium model (second-order association and first-

order dissociation) in which the binding constant was fixed to the value obtained from the titrations. The results are gathered in Table 1, and the corresponding energy barriers are listed in Table 2.

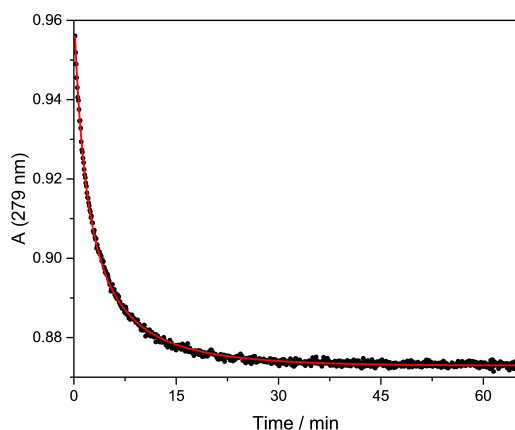


Figure 5. Time-dependent absorption changes at 279 nm recorded upon mixing DB24C8 and 4^+ in CH_2Cl_2 at 298 K. The red line represents the data fitting. Concentrations after mixing: $[\text{DB24C8}] = 1.6 \times 10^{-4} \text{ M}$, $[4^+] = 1.5 \times 10^{-4} \text{ M}$.

Table 2. Energetic parameters at 298 K, in kcal mol^{-1} .

| Guest ^[a] | Experimental | | Computed | |
|----------------------|---------------------------------|--|---|---|
| | ΔG° ^[b] | $\Delta G_{\text{in}}^\ddagger$ ^[c] | $\Delta G_{\text{out}}^\ddagger$ ^[c] | $\Delta G_{\text{out}}^\ddagger$ ^[d] |
| 1^+ | -8.6 | < 7.4 | < 16 | |
| 2^+ | | > 23 | | |
| 3^+ | | > 23 | | |
| 4^+ | -8.1 | 15.3 | 23.4 | |
| 5^+ | | > 23 | | |
| 6^+ | -7.1 | 16.0 | 23.1 | 19.8 |
| 7^+ | -8.0 | 15.3 | 23.3 | |
| 8^+ | | > 23 | | >100 |
| 9^+ | ^[e] | ^[e] | | |
| 10^+ | | > 23 | | |

[a] Shaded entries highlight the axles that undergo fast threading. [b] Association free energies, calculated from the measured K values (Table 1) using the expression $\Delta G^\circ = -RT \ln K$. [c] Activation free energies for the threading ($\Delta G_{\text{in}}^\ddagger$) and dethreading ($\Delta G_{\text{out}}^\ddagger$) processes, calculated from the measured rate constants (Table 1) using the relationships $\Delta G_{\text{in}}^\ddagger = -RT \ln(k_{\text{in}}/h/k_{\text{B}}T)$ and $\Delta G_{\text{out}}^\ddagger = -RT \ln(k_{\text{out}}/h/k_{\text{B}}T)$, respectively; R , h and k_{B} correspond respectively to the gas, Planck and Boltzmann constants. [d] Activation free energies for dethreading, determined from metadynamics simulations. [e] Data could not be obtained because of the poor solubility of axle 9^+ in CH_2Cl_2 . Measurements performed in acetonitrile indicate that this axle belongs to the “threading” category.

The first significant observation is that, while the threading of dibenzylammonium 1^+ into DB24C8 is immediate on the investigated time scale (the time resolution of our stopped-flow apparatus, dictated by the reactants mixing time, is 2 ms), the presence of two methyl substituents in the phenyl rings slows

down the assembly/disassembly process by at least five orders of magnitude (Table 1). Even more striking is the fact that (de)threading is allowed or prevented simply by changing the relative position of two methyl substituents on the phenyl ring (compare, for example, the behaviour of 2^+ and 3^+ with that of 4^+ and 6^+). Such an “all-or-nothing” effect, which was also observed in a previous investigation on related (pseudo)rotaxanes,^[22a] suggests that the (de)threading kinetics are determined by rigorous size complementarity requirements in which also the conformational freedom of the components presumably plays a role.

It is also interesting to note that the replacement of a methyl group for a methoxy group in the 4-position has very different consequences, depending on the position of the other methyl substituent. In fact, while in the case of the 2,4-derivatives a methoxy group in the place of a methyl in the 4-position seems to even accelerate the threading (6^+ versus 7^+), for 3,4-derivatives the presence of the 4-methoxy substituent prevents the formation of the complex (9^+ versus 10^+). The introduction of a further methoxy substituent in the 4-position of the 2,5-dimethyl species (4^+ versus 5^+) also blocks the threading.

The self-assembly of DB24C8 with the ammonium-type guests was also investigated in CD_3CN by ^1H NMR spectroscopy (Figure S16-S25). Spectrophotometric methods could not be used in this solvent because of the very low association under dilute conditions. Nonetheless, the NMR results confirm qualitatively the behaviour observed in dichloromethane, namely, the terminal units of 2^+ , 3^+ , 5^+ , 8^+ and 10^+ behave as real stoppers at room temperature. This observation suggests that the nature of the solvent, while likely contributing to the fine-tuning of the transition state(s), does not change significantly the (de)threading mechanism.

Computational studies

The experimental data clearly indicate that, with regard to threading, the ten structurally similar axles can be classified into two categories: “threading” (relatively fast formation of a pseudorotaxane; shaded entries in Tables 1 and 2) and “non-threading” (complex formation is not observed on the experimental timescale). To understand the molecular origin of this “all-or-nothing” behaviour, we modeled two representative examples of the “threading” and “non-threading” categories – the complexes of DB24C8 respectively with 6^+ and 8^+ – which differ only for the relative position of one methyl substituent. As illustrated in Figure 2, the gas-phase structures of the complexes are very similar because they are stabilized by hydrogen bonds and π - π stacking interactions of similar strength. The similarity between the two adducts is maintained in the equilibrium structures of the solvated complexes at 300 K (Figure 6a for 6^+ and 6d for 8^+).

Starting from these structures, we induced the dethreading of the two axles with *ab initio* metadynamics (see the SI and Movie S1).^[31] For each complex, we took the displacement of the axle with respect to the ring as a “reaction coordinate”, and computed the free energy during the transit of the axle through the macrocycle. We chose to model the dethreading process for the following reasons: (i) the ability of the terminal unit of the axle to act as a molecular “speed bump” in rotaxane-like architectures is essentially related to dethreading; (ii) in comparison with guest entrance, the exit process is less affected

by the solvent reorganization.^[11c] Hence, the markedly different dethreading behaviour of 6^+ and 8^+ may be directly correlated to their different interactions with the ring along the transit process, sketched in Figure 6b,c and 6e,f, respectively.

Clearly, the metadynamics simulations provide a yes/no outcome for the dethreading processes of 6^+ and 8^+ , respectively (Figure 7). Whereas the exit of 6^+ occurs at a relatively modest free energy cost (about 20 kcal mol⁻¹), over 100 kcal mol⁻¹ are not sufficient to expel 8^+ from the ring cavity (Table 2). Indeed, the maximum displacement of 8^+ along the simulated free energy path (Figure 6e,f) corresponds to situations where both phenyl rings are still inside the cavity. Conversely, in the dethreading profile of 6^+ , one of the phenyl moieties of the axle is entirely outside the ring already at the free energy maximum (Figure 6b), and the exit is essentially complete at the end of the simulation.

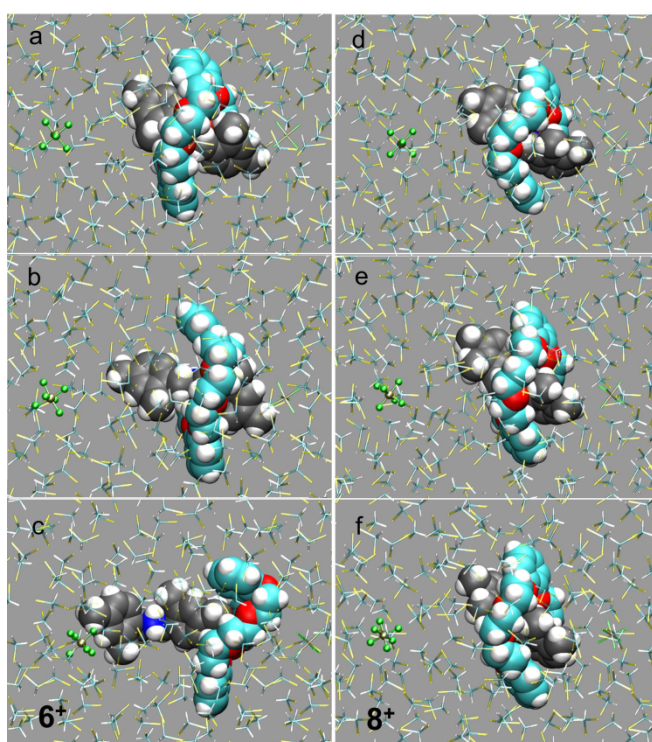


Figure 6. (a-c) Snapshots from the calculated dethreading path of the complex of DB24C8 with guest 6^+ : (a) initial state (threaded); (b) transition state (partially dethreaded); (c) final state (dethreaded). (d-f) Snapshots from the metadynamics simulation of the complex of DB24C8 with guest 8^+ , which predicted no dethreading. The atoms belonging to the complex are shown in a space-filling representation; color codes: C (ring) = cyan spheres; C (guest) = grey spheres; O = red; N = blue; H = white. Atoms of the solvent (CH_2Cl_2) and counterion (PF_6^-) are shown in a stick and ball-and-stick representation, respectively; color codes: C = cyan, Cl = yellow, H = white, P = dark grey, F = green.

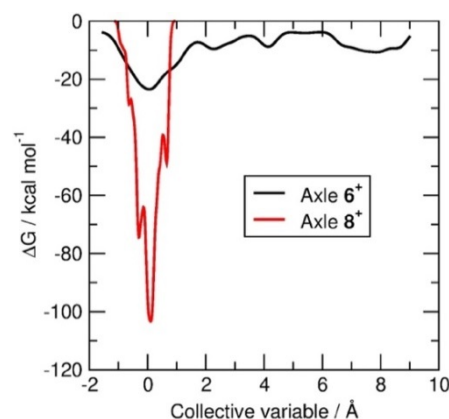


Figure 7. Free energy profile for the dethreading of the complexes of DB24C8 with guest 6^+ (black line) and 8^+ (red line) as a function of the displacement of the axle, defined by the collective variable. The latter is selected as the displacement of the 9 carbon atoms of one phenyl unit of the axle (including the C atoms of its two methyl substituents and of the methylene group) with respect to the 8 oxygen atoms of the macrocycle. The free energy cost associated to dethreading of 6^+ is 19.8 kcal mol⁻¹, while no dethreading can occur for 8^+ (free energy barrier above 100 kcal mol⁻¹).

Interestingly, the trajectories of the 6^+ and 8^+ complexes reveal that both axles tend to remain strongly hydrogen bonded to the macrocycle: in particular, 6^+ forms hydrogen bonds with different O atoms of the ring especially in the transition state of the exit process. Hence, the $[\text{N}^+-\text{H}\cdots\text{O}]$ hydrogen bonding interactions may be instrumental in assisting 6^+ to overcome the dethreading barrier. This mechanism, however, does not seem to work for 8^+ , which, despite forming hydrogen bonds with different DB24C8 oxygens along the simulation, is unable to leave the cavity.

In the case of 8^+ , we found that the ring enlarges significantly along its shorter axis to initiate the insertion of the end group of the guest. Yet such a distortion is not sufficient to enable the transit, which would require a substantial elongation of the ring along its main axis. In contrast, the deformation of DB24C8 during the exit process of 6^+ is far less pronounced, *i.e.*, dethreading of 6^+ occurs without significant elongations of the macrocycle along its long axis. Indeed, vibrational motions of the ring are smooth and synchronized with the movement of the axle – a common feature of transit movements in supramolecular systems and at molecule-material interfaces.^[32]

It remains to be understood why the elongation of DB24C8 along its main axis – never observed in our simulations – is apparently forbidden. By inspecting the vibrations of the ring, we found two normal modes – at 614 and 809 cm⁻¹ respectively – which achieve the maximum elongation of the ring (Figure 8 and Movies S2-S3). This deformation, which would be essential for the dethreading of 8^+ , is however not accessible at room temperature. Indeed, the vibrational modes responsible for ring elongation are too energetic with respect to $k_B T$, and would require the displacement and reorganization of a large number of solvent molecules. On the other hand, the dethreading of the $[\text{6-DB24C8}]^+$ complex is facilitated by lower energy vibrations (below 200 cm⁻¹) associated to more circular distortions of the ring, which enable the transit while preserving as much as possible the stabilizing host-guest interactions in the course of the exit process.

In order to provide further insight on the transition state (TS) governing the dethreading process of the $[6\text{-DB24C8}]^+$ complex, we performed a TS search using a different approach,^[33a] namely, via geometry optimization by adopting two different Density Functional Theory approximations: the PBE-D2^[31gh] one – which is the same adopted in the metadynamics study – and a hybrid functional (ωB97xd).^[33b] A continuum polarizable solvent model^[33c] was adopted for this approach (see the SI for details). Within the geometry optimization methodology, we obtained an activation free energy of $34.5\text{ kcal mol}^{-1}$ and $33.0\text{ kcal mol}^{-1}$ for the PBE-D2/D95(d,p) and $\omega\text{B97xd/D95(d,p)}$ level of theory, respectively. These values are higher than both the experimental data ($23.1\text{ kcal mol}^{-1}$) and the metadynamics results ($19.8\text{ kcal mol}^{-1}$; see Table S2). This point deserves some comments because it might shed light on the (de)threading mechanism. The main difference between the geometry optimization and the metadynamics approaches stems from the presence/absence of the CH_2Cl_2 solvent molecules in thermal equilibrium. Actually, in the real experiment, the supramolecular complex is caged by the solvent molecules, that may exchange kinetic energy with the complex via thermally induced collisions (Brownian motion). Such collisions, accounted for in the metadynamics simulations, provide a kinetic energy reservoir that the complex exploits to accomplish the energetically costly deformations needed for the axle-ring separation, thus effectively diminishing the dethreading barrier. Interestingly, such structural changes preferentially involve thermally accessible deformations, namely the ones which cause an elliptical to circular modification of the ethereal ring. Such a thermally accessible deformation allows for the exit of the axle 6^+ from the ring. This kind of circular deformation of the macrocycle is also predicted for the TS obtained via geometry optimization (see Figure 9 and SI Table S3, Scheme S1, and Movie S4), whose geometry is very similar to the structures in the activated complex region sampled by the metadynamics. However, at difference with the finite-temperature metadynamics simulation, in the optimized TS models no kinetic energy reservoir is present to facilitate the barrier crossing. Hence, while the presence/absence of solvent molecules does not seem to affect significantly the structure of the transition state, it plays indeed a key role on the kinetics of the process.

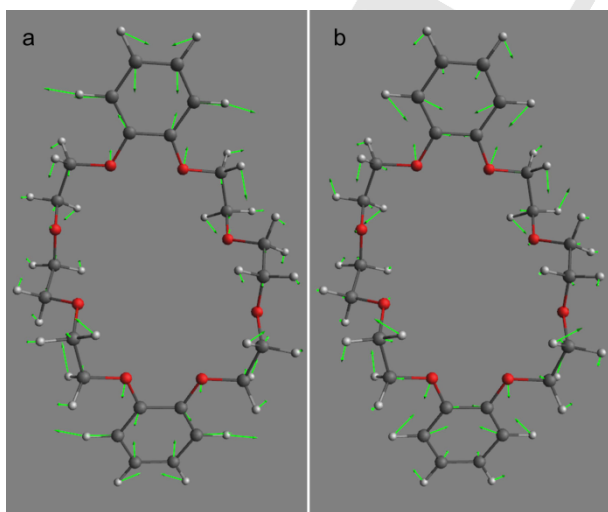


Figure 8. Vibrational modes of DB24C8 at 614 cm^{-1} (a) and at 809 cm^{-1} (b) which allow for the maximum elongation of the ring. Color codes: C = grey; O = red; H = white. The green arrows indicate the direction of the atomic displacements.

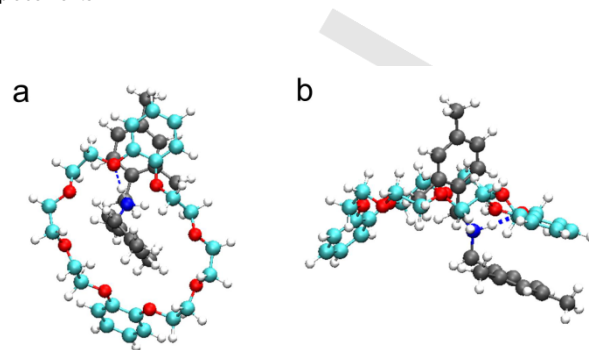


Figure 9. Optimized geometry of the transition state of the dethreading of the axle 6^+ from DB24C8, obtained with static quantum chemical calculation at the $\omega\text{B97xd/D95(d,p)}$ level of theory. a) Top view, highlighting the circular deformation of the ring; b) side view, highlighting the location of the transiting methyl group inside the DB24C8 cavity. Color codes: C (ring) = cyan; C (guest) = grey; O = red; N = blue; H = white. Blue dashed lines = hydrogen bonds.

Finally, we investigated the effect of the methoxy substituent in compounds 7^+ and 10^+ . Interestingly, replacing a methyl for a methoxy group on going from 6^+ to 7^+ does not change the threading behaviour of the axle, while the same change on going from 9^+ to 10^+ makes the latter compound unable to thread through the ring (Table 1). To rationalize such an observation, we simulated the dethreading of 10^+ from DB24C8 in the gas phase. We found that 10^+ could exit the ring only if the methoxy substituent performed an energetically costly rotation around its C–O axis, bringing the CH_3 group in close contact with the adjacent methyl substituent (SI, Figure S2). As the passage of 10^+ through the ring would require energetically unfavourable conformational changes, we conclude that this process should be very unlikely, in agreement with the experimental results.

Discussion

We can now try to generalize the findings reported above and explain the belonging of the guests to the “threading” and “non-threading” categories. First, all investigated guests except 5^+ have two more substituents on each phenyl ring with respect to dibenzylammonium (1^+). In these compounds, the “threading” or “non-threading” behaviour is determined not only by the relative position of the two substituents on the phenyl ring that is being traversed, but also by their position with respect to the axis individuated by the C–C bond of the methylene substituent attached to the ammonium centre (blue dashed line in Figure 10). As the methylene group must necessarily pass through the cavity during threading or dethreading, this axis is somehow related to the transit direction.

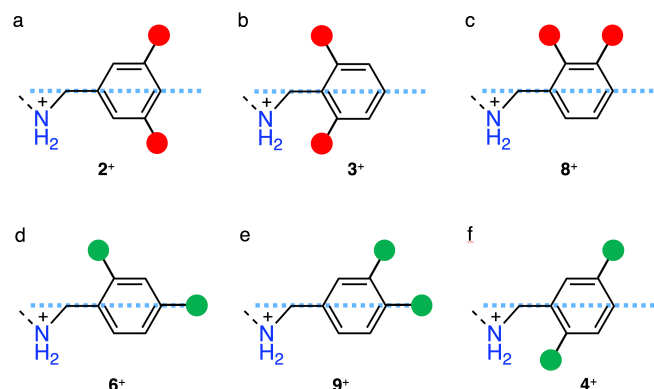


Figure 10. Correlation between the substitution pattern and the kinetic behaviour of DB24C8 threading for symmetric dibenzylammonium-type guest bearing two methyl substituents in each phenyl ring. (a-c) “Non-threading” category, methyl substituents shown in red. (d-f) “Threading” category, methyl substituents shown in green. The blue dashed line shows the axis related to the transit direction.

When the two substituents on each phenyl ring are methyl groups, a rather simple correlation exists between the kinetic behaviour of the guests and the substitution pattern (Figure 10). Specifically, when the two methyl substituents are positioned symmetrically with respect to the principal axis mentioned in the previous paragraph (Figure 10a,b, compounds 2^+ and 3^+), or adjacent and off-axis (Figure 10c, compound 8^+), the guest belongs to the “non-threading” category. When one of the two methyl groups is located on-axis, the position of the other substituent is irrelevant and the guest is of the “threading” type (Figure 10d,e, compounds 6^+ and 9^+). Threading can also be obtained when the two methyl groups are off-axis but neither adjacent nor symmetrically arranged (Figure 10f, compound 4^+), probably because in this pattern the steric encumbrances of the two groups along the (de)threading coordinate cannot add up effectively.

When the on-axis methyl group is replaced by a methoxy, which has a larger size and conformational freedom, our results seem to indicate that the distance between the two substituents becomes crucial. Probably, the combined presence of the methyl substituent and of particular conformations of the methoxy group can cause a significant steric hindrance only if the two groups are nearby, as in 10^+ , in line with the computational results. This effect vanishes in 7^+ , wherein the two substituents are more spaced.

Conclusion

We have employed a combined experimental and computational approach to investigate the (de)threading of a library of ten dibenzylammonium-type axles with dibenzo[24]crown-8 – a most exploited self-assembling motif in supramolecular chemistry, mechanically interlocked molecules and molecular machines, with applications in catalysis and materials science. The axles have been designed and synthesized to study the effect of small structural variations of their phenyl end groups on the threading and dethreading rates. We found that the axles can be clearly divided in two categories: those that undergo relatively fast threading, and those that are completely unable to pierce the

ring. Remarkably, changing the position of just one methyl substituent on the terminal phenyl rings is sufficient to switch the category of the axle.

Computational modelling of the dethreading process revealed that hydrogen bonding between the host and the guest is still present in the transition state, and that vibrational modes that cause an extension of the macrocyclic cavity play a key role. The kinetic energy reservoir provided by the solvent molecules in thermal equilibrium facilitates the activation of the (pseudo)-rotaxane for dethreading, allowing for ring deformations. However, only elongations of the ring along its shorter axis are accessible at room temperature; in other words, the crown cavity cannot become more elliptical. This is probably the reason for the all-or-nothing kinetic selectivity observed for structurally similar axles – namely, the fine mechanics of the self-assembly process is actually ruled by quantum mechanics. From these insights, simple rules correlating the kinetic behaviour with the substitution pattern have been derived.

The present work has provided a detailed molecular understanding of the (de)threading reactions and has enriched on a fundamental basis the generally accepted phenomenological picture. By studying a representative class of molecular components, rational guidelines for the design of pseudostoppers or “speed bumps”, necessary for the realization of molecular mechanical switches and motors with predetermined dynamic features have been formulated. Jointly with these practical rules, the fundamental knowledge acquired on the kinetic behaviour may be extended to other self-assembling architectures in which the mechanical fit of the components can give rise to technologically relevant functionalities.

Acknowledgements

Financial support from the EU (ERC AdG “Leaps” n. 692981), MIUR (Fare “Ampli” R16S9XXKX3, Prin “Nemo” 20173L7W8K), and University of Insubria (FAR2018) is gratefully acknowledged. L.C. and E.F. acknowledge the King Abdullah University of Science and Technology (KAUST) Supercomputing Laboratory (KSL) for providing computational resources on Shaheen II Cray XC40 Supercomputer within project k1345.

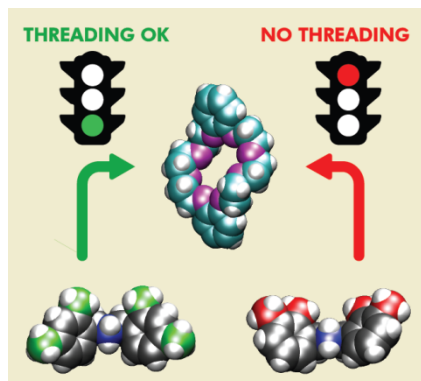
Keywords: kinetics • metadynamics • molecular machine • supramolecular chemistry • rotaxane

- [1] a) V. Balzani, A. Credi, M. Venturi *Molecular Devices and Machines – Concepts and Perspectives for the Nanoworld*. Wiley-VCH, Weinheim, **2008**; b) *Comprehensive Supramolecular Chemistry II*. (Ed. J. L. Atwood), Elsevier, Oxford, **2017**; c) A. A. Gakh, *Molecular Devices: An Introduction to Technomimetics and its Biological Applications*. Wiley, Hoboken, **2018**.
- [2] a) V. Balzani, *Small* **2005**, *1*, 278-283; b) X. Ma, H. Tian, *Chem. Soc. Rev.* **2010**, *39*, 70-80; c) S. Erbas-Cakmak, D. A. Leigh, C. T. McTernan, A. L. Nussbaumer, *Chem Rev.* **2015**, *115*, 10081-10206; d) D. B. Amabilino, D. K. Smith, J. W. Steed, *Chem. Soc. Rev.* **2017**, *46*, 2404-2420; e) S. Corra, M. Curcio, M. Baroncini, S. Silvi, A. Credi, *Adv. Mater.* **2020**, *32*, e1906064.
- [3] R. A. L. Jones *Soft Machines: Nanotechnology and Life*. Oxford University Press, Oxford, **2008**.

- [4] C. O. Dietrich-Buchecker, J.-P. Sauvage, J.-P. Kintzinger, *Tetrahedron Lett.* **1983**, *24*, 5095-5098.
- [5] C. J. Bruns, J. F. Stoddart, *The Nature of the Mechanical Bond: from Molecules to Machines*. Wiley, Hoboken, **2016**.
- [6] a) P. R. Ashton, I. Baxter, M. C. T. Fyfe, F. M. Raymo, N. Spencer, J. F. Stoddart, A. J. P. White, D. J. Williams *J. Am. Chem. Soc.* **1998**, *120*, 2297-2307. b) J. O. Jeppesen, S. A. Vignon, J. F. Stoddart *Chem. Eur. J.* **2003**, *9*, 4611-4625.
- [7] a) P. R. Ashton, M. Belohradsky, D. Philp, J. F. Stoddart, *J. Chem. Soc. Chem. Commun.* **1993**, 1269-1274; b) M. Asakawa, P. R. Ashton, R. Ballardini, V. Balzani, M. Belohradsky, M. T. Gandolfi, O. Kocian, L. Prodi, F. M. Raymo, J. F. Stoddart, M. Venturi *J. Am. Chem. Soc.* **1997**, *119*, 302-310.
- [8] a) M. A. Bolla, J. Tiburcio, S. J. Loeb *Tetrahedron* **2008**, *64*, 8423-8427; b) A. J. McConnell, P. D. Beer *Chem. Eur. J.* **2011**, *17*, 2724-2733; c) Y. Akae, H. Okamura, Y. Koyama, T. Arai, T. Takata *Org. Lett.* **2012**, *14*, 2226-2229; d) A. B. C. Deutman, S. Varghese, M. Moalin, J. A. A. W. Elmans, A. E. Rowan, R. J. M. Nolte *Chem. Eur. J.* **2015**, *21*, 360-370.
- [9] a) Y. Kawaguchi, A. Harada *J. Am. Chem. Soc.* **2000**, *122*, 3797-3798; b) M. Hmadeh, A. C. Fahrenbach, S. Basu, A. Trabolsi, D. Benítez, H. Li, A.-M. Arbrecht-Gary, M. Elhabiri, J. F. Stoddart *Chem. Eur. J.* **2011**, *17*, 6076-6087; c) A. E. Kaifer, W. Li, S. Silvi, V. Sindelar, *Chem. Commun.* **2012**, *48*, 6693-6695; d) A. C. Catalán, J. Tiburcio, *Chem. Commun.* **2016**, *52*, 9526-9529.
- [10] a) M. Venturi, S. Dumas, V. Balzani, J. Cao, J. F. Stoddart *New J. Chem.* **2004**, *28*, 1032-1037; b) K.-D. Zhang, X. Zhao, G.-T. Wang, Y. Liu, Y. Zhang, H.-J. Lu, X.-K. Jian, Z.-T. Li *Tetrahedron* **2012**, *68*, 4517-4527; c) A. Arduini, R. Bussolati, A. Credi, A. Secchi, S. Silvi, M. Semeraro, M. Venturi *J. Am. Chem. Soc.* **2013**, *135*, 9924-9930; d) X. Wang, B. Wicher, Y. Ferrand, I. Huc *J. Am. Chem. Soc.* **2017**, *139*, 9350-9358; e) B. Riss-Yaw, C. Clavel, Ph. Laurent, F. Coutrot *Chem. Commun.* **2017**, *53*, 10874-10877.
- [11] a) M. Baroncini, S. Silvi, M. Venturi, A. Credi *Chem. Eur. J.* **2010**, *16*, 11580-11587; b) A. Arduini, R. Bussolati, A. Credi, S. Monaco, A. Secchi, S. Silvi, M. Venturi *Chem. Eur. J.* **2012**, *18*, 16203-16213; c) G. Tabacchi, S. Silvi, M. Venturi, A. Credi, E. Fois *ChemPhysChem* **2016**, *17*, 1913-1919; d) D. A. Leigh, L. Pirvu, F. Schaufelberger, D. J. Tettlow, L. Zhang, *Angew. Chem. Int. Ed.* **2018**, *57*, 10484-10488.
- [12] M. Baroncini, S. Silvi, A. Credi *Chem. Rev.* **2020**, *120*, 200-268.
- [13] R. D. Astumian *Phys. Chem. Chem. Phys.* **2007**, *9*, 5067-5083.
- [14] a) J. V. Hernandez, E. R. Kay, D. A. Leigh *Science* **2004**, *306*, 1532-1537; b) S. Erbas-Cakmak, S. D. P. Fielden, U. Karaca, D. A. Leigh, C. T. McTernan, D. J. Tettlow, M. R. Wilson *Science* **2017**, *358*, 340-343.
- [15] a) C. Cheng, P.R. McGonigal, W.-G. Liu, H. Li, N. A. Vermeulen, C. Ke, M. Frascioni, C. L. Stern, W. A. Goddard III, J. F. Stoddart *J. Am. Chem. Soc.* **2014**, *136*, 14702-14705; b) C. Cheng, P. R. McGonigal, S. T. Schneebeli, H. Li, N. A. Vermeulen, C. Ke, J. F. Stoddart *Nat. Nanotechnol.* **2015**, *10*, 547-553.
- [16] C. Pezzato, M. T. Nguyen, D. J. Kim, A. Anamimoghadam, L. Mosca, J. F. Stoddart *Angew. Chem. Int. Ed.* **2018**, *57*, 9325-9329.
- [17] a) M. Baroncini, S. Silvi, M. Venturi, A. Credi *Angew. Chem. Int. Ed.* **2012**, *51*, 4223-4226; b) G. Ragazzon, M. Baroncini, S. Silvi, M. Venturi, A. Credi *Nat. Nanotechnol.* **2015**, *10*, 70-75.
- [18] a) S. Chen, Y. Wang, T. Nie, C. Bao, C. Wang, T. Xu, Q. Lin, D.-H. Qu, X. Gong, Y. Yang, L. Zhu, H. Tian *J. Am. Chem. Soc.* **2018**, *140*, 17992-17998; b) A. Credi *Angew. Chem. Int. Ed.* **2019**, *58*, 4108-4110.
- [19] For seminal investigations on directional control of threading and dethreading movements, see: a) T. Oshikiri, Y. Takashima, H. Yamaguchi, A. Harada *Chem. Eur. J.* **2007**, *13*, 7091-7098; b) J. W. Park, H. J. Song, Y. J. Cho, K. K. Park *J. Phys. Chem. C* **2007**, *111*, 18605-18614; c) A. Arduini, R. Bussolati, A. Credi, G. Faimani, S. Garaudée, A. Pochini, A. Secchi, M. Semeraro, S. Silvi, M. Venturi, *Chem. Eur. J.* **2009**, *15*, 3230-3242.
- [20] a) Y. Kohsaka, K. Nakazono, Y. Koyama, S. Asai, T. Takata *Angew. Chem. Int. Ed.* **2011**, *50*, 4872-4875; b) H. Sato, D. Aoki, T. Takata, *Chem. Asian J.* **2018**, *13*, 785-789.
- [21] P. R. Ashton, M. C. T. Fyfe, S. K. Hickingbottom, J. F. Stoddart, A. J. P. White, D. J. Williams *J. Chem. Soc. Perkin Trans. 2* **1998**, 2117-2128.
- [22] a) F. M. Raymo, K. N. Houk, J. F. Stoddart *J. Am. Chem. Soc.* **1998**, *120*, 9318-9322; b) A. Affeld, G. M. Hübner, C. Seel, C. A. Schalley *Eur. J. Org. Chem.* **2001**, 2877-2890; c) Y. Tokunaga, T. Goda, N. Wakamatsu, R. Nakata, Y. Shimomura *Heterocycles* **2006**, *68*, 5-10; d) P. R. McGonigal, H. Li, C. Cheng, S. T. Schneebeli, M. Frascioni, L. S. Witus, J. F. Stoddart *Tetrahedron Lett.* **2015**, *56*, 3591-3594; e) M. Quiroga, M. Parajó, P. Rodríguez-Dafonte, L. García-Río *Langmuir* **2016**, *32*, 6367-6375; f) T. Legigan, B. Riss-Yaw, C. Clavel, F. Coutrot *Chem. Eur. J.* **2016**, *22*, 8835-8847; g) A. Martínez-Cuevza, F. Morales, G. R. Marley, A. Lopez-Lopez, J. C. Martínez-Costa, D. Bautista, M. Alajarin, J. Berna *Eur. J. Org. Chem.* **2019**, 3480-3488.
- [23] a) A. G. Kolchinski, D. H. Busch, N. W. Alcock *J. Chem. Soc. Chem. Commun.* **1995**, 1289-1291; b) P. R. Ashton, P. J. Campbell, E. J. T. Chrystal, P. T. Glink, S. Menzer, D. Philp, N. Spencer, J. F. Stoddart, P. A. Tasker, D. J. Williams *Angew. Chem. Int. Ed. Engl.* **1995**, *34*, 1865-1869; c) P. R. Ashton, E. J. T. Chrystal, P. T. Glink, S. Menzer, C. Schiavo, N. Spencer, J. F. Stoddart, P. A. Tasker, A. J. P. White, D. J. Williams *Chem. Eur. J.* **1996**, *2*, 709-728.
- [24] a) S. J. Cantrill, A. R. Pease, J. F. Stoddart *J. Chem. Soc. Dalton Trans.* **2000**, 3715-3734; b) Z. Bo, W. Feng, S. Dong, F. Huang *Chem. Soc. Rev.* **2012**, *41*, 1621-2636; c) Z. Liu, S. K. M. Nalluri, J. F. Stoddart *Chem. Soc. Rev.* **2017**, *46*, 2459-2478.
- [25] See, e.g.: a) A. G. Kolchinski, N. W. Alcock, R. A. Roesner, D. H. Busch *Chem. Commun.* **1998**, 1437-1438; b) N. Yamaguchi, H. W. Gibson *Angew. Chem. Int. Ed. Engl.* **1999**, *38*, 143-147; c) V. Balzani, M. Clemente-Léon, A. Credi, J. N. Lowe, J. Badjić, J. F. Stoddart, D. J. Williams *Chem. Eur. J.* **2003**, *9*, 5348-5360; d) Y. Furusho, T. Oku, T. Hasegawa, A. Tsuboi, N. Kihara, T. Takata *Chem. Eur. J.* **2003**, *9*, 2895-2903; e) B. Ferrer, G. Rogez, A. Credi, R. Ballardini, M. T. Gandolfi, V. Balzani, Y. Liu, H.-R. Tseng, J. F. Stoddart *Proc. Natl. Acad. Sci. U.S.A.* **2006**, *103*, 18411-18416; f) W. Jiang, K. Nowosinski, N. L. Löw, E. V. Dzyuba, F. Klautzsch, A. Schafer, J. Huuskonen, K. Rissanen, C. A. Schalley *J. Am. Chem. Soc.* **2011**, *134*, 1860-1868; g) V. Bleve, P. Franchi, E. Kostanteli, L. Gualandi, S. M. Goldup, E. Mezzina, M. Lucarini, *Chem. Eur. J.* **2018**, *24*, 1198-1203; h) M. Zhang, G. De Bo *J. Am. Chem. Soc.* **2019**, *141*, 15879-15883.
- [26] See, e.g.: a) W. Jiang, A. Schafer, P. C. Mohr, C. A. Schalley *J. Am. Chem. Soc.* **2010**, *132*, 2309-2320; b) K. Nakazono, T. Ishino, T. Takashima, D. Saeki, D. Natsui, N. Kihara, T. Takata *Chem. Commun.* **2014**, *50*, 15341-15344; c) S. Chao, C. Romuald, E. Fournel-Marotte, C. Clavel, F. Coutrot *Angew. Chem. Int. Ed.* **2014**, *53*, 6914-6919; d) Z. Chen, D. Aoki, S. Uchida, H. Marubayashi, S. Nojima, T. Takata *Angew. Chem. Int. Ed.* **2016**, *55*, 2778-2781; e) D. Aoki, G. Aibara, S. Uchida, T. Takata *J. Am. Chem. Soc.* **2017**, *139*, 6791-6794; f) S. D. P. Fielden, D. A. Leigh, C. T. McTernan, B. Pérez-Saavedra, I. J. Vitorica-Yrezabal *J. Am. Chem. Soc.* **2018**, *140*, 6049-6052.
- [27] See, e.g.: a) C. R. South, K. C.-F. Leung, D. Lanari, J. F. Stoddart, M. Weck *Macromolecules* **2006**, *39*, 3738-3744; b) M. Zhang, D. Xu, X. Yan, J. Chen, S. Dong, B. Zheng, F. Huang *Angew. Chem. Int. Ed.* **2012**, *51*, 7011-7015; c) S. Dong, B. Zheng, D. Xu, X. Yan, M. Zhang, F. Huang *Adv. Mater.* **2012**, *24*, 3191-3195; d) J.-M. Han, Y.-H. Zhang, X.-Y. Wang, C.-J. Liu, J.-Y. Wang, J. Pei *Chem. Eur. J.* **2012**, *19*, 1502-1510; e) X. Yan, T. R. Cook, J. B. Pollock, P. Wei, Y. Zhang, Y. Yu, F. Huang, P. J. Stang *J. Am. Chem. Soc.* **2014**, *136*, 4460-4463.
- [28] a) V. Blanco, A. Carlone, K. D. Haenni, D. A. Leigh and B. Lewandowski *Angew. Chem. Int. Ed.* **2012**, *51*, 5166-5169; b) V. Blanco, D. A. Leigh, U. Lewandowska, B. Lewandowski, V. Marcos *J. Am. Chem. Soc.* **2014**, *136*, 15775-15780; c) K. Eichstaedt, J. Jaramillo-Garcia, D. A. Leigh, V. Marcos, S. Pisano, T. A. Singleton, *J. Am. Chem. Soc.* **2017**, *139*, 9376-9381; d) C. Biagini, S. D. P. Fielden, D. A. Leigh, F. Schaufelberger, S. Di Stefano, D. Thomas, *Angew. Chem. Int. Ed.* **2019**, *58*, 9876-9880.
- [29] See, e.g.: a) J. D. Badjić, V. Balzani, A. Credi, S. Silvi, J. F. Stoddart *Science* **2004**, *303*, 1845-1849; b) V. Serrelli, C.-F. Lee, E. R. Kay, D. A. Leigh *Nature* **2007**, *445*, 523-527; c) F. Coutrot, C. Romuald, E. Busseron *Org. Lett.* **2008**, *10*, 3741-3744; d) J. Wu, K. C.-F. Leung, D. Benítez, J.-Y. Han, S. J. Cantrill, L. Fang, J. F. Stoddart *Angew. Chem. Int. Ed.* **2008**, *47*, 7470-7474; e) G. Ragazzon, C. Schäfer, P. Franchi, S. Silvi, B. Colasson, M. Lucarini, A. Credi *Proc. Natl. Acad. Sci. U. S.*

- A. **2018**, *115*, 9385-9390; f) Q. Zhang, S.-J. Rao, T. Xie, X. Li, T. Xu, D. Li, D.-H. Qu, Y. Long, H. Tian *Chem* **2018**, *4*, 2670-2684; g) S. Corra, C. de Vet, J. Groppi, M. La Rosa, S. Silvi, M. Baroncini, A. Credi *J. Am. Chem. Soc.* **2019**, *141*, 9129-9133; h) A. H. G. David, R. Casares, J. M. Cuerva, A. G. Campaña, V. Blanco *J. Am. Chem. Soc.* **2019**, *141*, 18064-18074.
- [30] a) M. Clemente-León, C. Pasquini, V. Hebbe-Viton, J. Lacour, A. Dalla Cort, A. Credi, *Eur. J. Inorg. Chem.* **2006**, 105-112; b) H. W. Gibson, J. W. Jones, L. N. Zakharov, A. L. Rheingold, C. Slebodnick, *Chem. Eur. J.* **2011**, *17*, 3192-3206.
- [31] a) A. Laio, M. Parrinello, *Proc. Natl. Acad. Sci. U.S.A.* **2002**, *20*, 12562-12566; b) M. Iannuzzi, A. Laio, M. Parrinello, *Phys. Rev. Lett.* **2003**, *90*, 238302; c) A. Barducci, M. Bonomi, M. Parrinello, *WIREs Comput. Mol. Sci.* **2011**, *1*, 826-843; d) P. Raiteri, G. Bussi, C. S. Cucinotta, A. Credi, J. F. Stoddart, M. Parrinello, *Angew. Chem. Int. Ed.* **2008**, *47*, 3536-3539; e) D. M. Santiburcio, D. Marx, *Chem. Sci.* **2017**, *8*, 3444-3452; f) P. Ahlawat, M. I. Dar, P. Piaggi, M. Grätzel, M. Parrinello, U. Rothlisberger, *Chem. Mater.* **2020**, *32*, 529-536; g) J. P. Perdew, K. Burke, M. Ernzerhof, *Phys. Rev. Lett.* **1996**, *77*, 3865; h) S. Grimme, *J. Comp. Chem.* **2006**, *27*, 1787-1799; i) R. Car, M. Parrinello, *Phys. Rev. Lett.* **1985**, *55*, 2471; j) S. R. Billeter, A. Curioni, W. Andreoni, *Comput. Mater. Science* **2003**, *27*, 437-445; k) CPMD code, <http://www.cpmd.org>. Copyright IBM Corp. 1990-2019, MPI für Festkörperforschung Stuttgart, 1997-2001.
- [32] See, e.g.: a) f) E. Fois, G. Tabacchi, D. Barreca, A. Gasparotto, E. Tondello, *Angew. Chem. Int. Ed.* **2010**, *49*, 1944-1948; b) E. Fois, G. Tabacchi, G. Calzaferri, *J. Phys. Chem. C* **2012**, *116*, 16784-16799; c) X. Zhou, T. A. Wesolowski, G. Tabacchi, E. Fois, G. Calzaferri, A. Devaux, *Phys. Chem. Chem. Phys.* **2013**, *15*, 159-167; d) G. Tabacchi, E. Fois, G. Calzaferri, *Angew. Chem. Int. Ed.* **2015**, *54*, 11112-11116; e) G. Tabacchi, G. Calzaferri, E. Fois, *Chem. Commun.* **2016**, *52*, 11195-11198; f) R. Arletti, E. Fois, L. Gigli, G. Vezzalini, S. Quartieri, G. Tabacchi, *Angew. Chem. Int. Ed.* **2017**, *56*, 2105-2109; g) G. Tabacchi, *ChemPhysChem* **2018**, *19*, 1249-1297; h) G. Tabacchi, M. Fabbiani, L. Mino, G. Martra, E. Fois, *Angew. Chem. Int. Ed.* **2019**, *58*, 12431-12434.
- [33] a) Gaussian 09, Revision B.01, M. J. Frisch et al; b) D. Chai, M. Head-Gordon, *Phys. Chem. Chem. Phys.* **2008**, *10*, 6615-6620; c) J. Tomasi, B. Mennucci, R. Cammi, *Chem. Rev.* **2005**, *105*, 2999-3094.

Entry for the Table of Contents



Fine mechanics: with a systematic experimental and computational investigation, we explain why tiny structural changes in the extremities of a molecular axle can allow or prevent its insertion in the cavity of a macrocycle. These results provide guidelines to design interlocked molecules with predetermined dynamic features, that can be used to make nanostructured machines, motors and materials.

Institute and/or researcher Twitter usernames: @erc_leaps, @UniboMagazine; @fe_ga_to; @BL76276